



## Thermal inactivation, denaturation and aggregation of mitochondrial aspartate aminotransferase

Nikolay V. Golub<sup>a</sup>, Kira A. Markossian<sup>a,\*</sup>, Natallia V. Kasilovich<sup>b</sup>, Mikhail V. Sholukh<sup>b</sup>, Victor N. Orlov<sup>c</sup>, Boris I. Kurganov<sup>a</sup>

<sup>a</sup> Bach Institute of Biochemistry, Russian Academy of Sciences, Moscow, Russia

<sup>b</sup> Belarusian State University, Minsk, Belarus

<sup>c</sup> Belozersky Institute of Physico-Chemical Biology, Moscow State University, Moscow, Russia

### ARTICLE INFO

#### Article history:

Received 6 December 2007

Received in revised form 31 March 2008

Accepted 1 April 2008

Available online 10 April 2008

#### Keywords:

Mitochondrial aspartate aminotransferase

Denaturation

Inactivation

Aggregation

### ABSTRACT

A comparative study of thermal denaturation and inactivation of aspartate aminotransferase from pig heart mitochondria (mAAT) has been carried out (10 mM Na phosphate buffer, pH 7.5). Analysis of the data on differential scanning calorimetry shows that thermal denaturation of mAAT follows the kinetics of irreversible reaction of the first order. The kinetics of thermal inactivation of mAAT follows the exponential law. It has been shown that the inactivation rate constant ( $k_{in}$ ) is higher than the denaturation rate constant ( $k_{den}$ ). The  $k_{in}/k_{den}$  ratio decreases from  $28.8 \pm 0.1$  to  $1.30 \pm 0.09$  as the temperature increases from 57.5 to 77 °C. The kinetic model explaining the discrepancy between the inactivation and denaturation rates has been proposed. The size of the protein aggregates formed at heating of mAAT at a constant rate ( $1\text{ °C min}^{-1}$ ) has been characterized by dynamic light scattering.

© 2008 Elsevier B.V. All rights reserved.

### 1. Introduction

Aspartate aminotransferase (EC 2.6.1.1), a homodimeric, pyridoxal 5'-phosphate (PLP)-dependent enzyme, exists in two distinct forms in higher eukaryotes, one located in the cytosol and the other in the mitochondria [1]. The enzyme contains one molecule of PLP bound to each of the two identical active sites. A single polypeptide chain comprising each subunit folds into three distinct regions: an N-terminal extended arm that interacts with the neighboring subunit, a small domain that changes its conformation during catalysis and a large domain that contains most of the residues involved in cofactor binding [2]. The active site is adjacent to both the domain and the subunit interfaces [2]. It is formed by loops of polypeptide from the large and small domains of its own subunit and by a few residues from the large domain of the adjacent subunit. The coenzyme PLP is attached to the active site by a covalent link (Schiff base) to the side-chain of Lys258. The functionally independent active sites lie at the interface between the small and large domains on the opposite sides of the dimeric molecule [3]. Since each active site is composed of residues from both subunits, only dimeric enzyme shows catalytic activity. The monomeric form of the enzyme is catalytically inactive [4].

The dimeric cytosolic isoenzyme with molecular mass of  $93.0 \pm 2.8$  kDa and dimeric mitochondrial isoenzyme with molecular mass of  $91.2 \pm 2.7$  kDa [5] are structurally related, with approximately 48% identity of amino acid sequence [6], but they exhibit considerable differences in stability to denaturing agents [7,8] and sensitivity to thermal denaturation [9]. The melting temperatures of the two isoenzymes at pH 7.5 as determined by differential scanning calorimetry (DSC) were 83 and 68 °C for the cytosolic and mitochondrial isoenzymes, respectively [9]. Mitochondrial aspartate aminotransferase (mAAT) is inactivated irreversibly at heating, the inactivation being a first-order process [10,11]. During heating aggregates of the enzyme are formed. Light scattering data at 360 nm have shown that the increase in turbidity is more rapid at higher temperature [10].

In the present work we have compared the rates of inactivation and denaturation of mAAT from pig heart mitochondria in the temperature interval from 50 to 77 °C. Denaturation of mAAT was studied by DSC. Inactivation and denaturation of mAAT proceed as irreversible reactions of the first order. The obtained results have shown that the active site reveals lesser stability in comparison with that of the protein globule as a whole. Thermal aggregation of mAAT has been studied by dynamic light scattering (DLS) under the regime, wherein the temperature was elevated at a rate of  $1\text{ °C min}^{-1}$ . When comparing the increment in the light scattering intensity ( $I$ ) and the portion of the denatured protein ( $\gamma_{den}$ ), we observed that the normalized  $I$  values ( $I/I_{lim}$ ;  $I_{lim}$  is the limiting value of  $I$  at  $\gamma_{den}=1$ ) exceed the  $\gamma_{den}$  values.

\* Corresponding author. Fax: +7 495 954 2732.

E-mail address: [markossian@inbi.ras.ru](mailto:markossian@inbi.ras.ru) (K.A. Markossian).

Abbreviations: DLS, dynamic light scattering; DSC, differential scanning calorimetry; mAAT, mitochondrial aspartate aminotransferase; PLP, pyridoxal 5'-phosphate.

## 2. Materials and methods

### 2.1. Materials

L-aspartic acid, malate dehydrogenase (MDH), NADH and  $\alpha$ -ketoglutaric acid were purchased from Sigma; CM-32 cellulose was from Whatman; DE-sepharose (fast flow) were from Pharmacia; Macro-Prep ceramic hydroxyapatite was from Bio-Rad; pyridoxal 5'-phosphate (PLP) and 2-mercaptoethanol were from Loba Chemie.

All solutions for the experiments were prepared using deionized water obtained with Easy-Pure II RF system (Barnstead, USA).

### 2.2. Purification of mAAT

The enzyme was purified according to Barra et al. [12] with several modifications. Freshly obtained pig hearts were minced and 1.5 kg of the material was homogenized in 1.8 L buffer A (10 mM K-phosphate buffer, pH 6.8, containing 10 mM glutaric acid, 5  $\mu$ M PLP, 0.5 mM EDTA and 0.2 mM 2-mercaptoethanol). Insoluble material was collected by centrifugation at 2500 g and re-extracted with buffer A two times. The combined supernatants were dialyzed against buffer A. The dialyzed solution was clarified by centrifugation at 16900 g and then applied on the column (5 $\times$ 25 cm) of CM-cellulose equilibrated with 10 mM K-phosphate buffer, pH 6.8. The mitochondrial enzyme was eluted from the column using buffer A containing 0.25 mM NaCl. The active fractions were combined and dialyzed overnight against buffer A. The dialyzed solution was applied to a column (3.6 $\times$ 30 cm) of CM-cellulose equilibrated with 10 mM K-phosphate buffer, pH 6.8. The mAAT was eluted using a salt gradient with buffer A containing 10 mM NaCl (500 mL) in the mixing chamber and buffer A containing 125 mM NaCl (500 mL) in the reservoir. Flow rates of about 300 mL h<sup>-1</sup> were used. The active fraction was dialyzed overnight against buffer B (10 mM K-phosphate buffer, pH 8.0, containing 1 mM  $\alpha$ -ketoglutaric acid, 5  $\mu$ M PLP and 0.2 mM 2-mercaptoethanol). Then the enzyme solution was applied on DE-sepharose column (2.5 $\times$ 25 cm) concatenated with the hydroxyapatite column (1.6 $\times$ 20 cm); both columns were equilibrated with buffer A. After washing with the same buffer columns were disconnected and mAAT was eluted from hydroxyapatite column in AKTA FPLC system under the following conditions: buffer B (10 mM K-phosphate buffer, pH 8.0, containing 1 mM  $\alpha$ -ketoglutaric acid, 5  $\mu$ M PLP and 0.2 mM 2-mercaptoethanol), buffer C (0.5 M K-phosphate buffer, pH 8.0, containing 10 mM glutaric acid, 5  $\mu$ M PLP and 0.2 mM 2-mercaptoethanol); gradient slope was 10 column volumes of 10–50% buffer C. Fractions containing enzyme were pooled and concentrated. Application of DE-sepharose/hydroxyapatite in the final step of tandem chromatography allowed us to obtain homogeneous preparation of mAAT according to SDS-PAGE with activity not less than 229 $\pm$ 10 U mg<sup>-1</sup>.

Protein concentration was determined according to Peterson [13] or from the absorbance at 280 nm using the extinction coefficient  $A_{280}^{1\%} = 14.0$  [12].

### 2.3. Assay of mAAT

mAAT activity was measured at 25 °C by coupling the enzyme reaction with malate dehydrogenase (MDH) and subsequent monitoring NADH oxidation at 340 nm on Cary 50 Bio UV/Visible spectrophotometer [14]. The reaction mixture (1 mL) contained 0.05 M K-phosphate buffer, pH 6.8, 20 mM  $\alpha$ -ketoglutaric acid, 0.2 mM NADH,  $\sim$ 3 U ml<sup>-1</sup> MDH and an appropriate amount of the sample. The reaction was started by the addition of L-aspartate to a final concentration of 10 mM. One unit of the enzyme activity was defined as the amount of the enzyme that is required for the formation of 1  $\mu$ mol of the product per 1 min under the above conditions.

### 2.4. Calorimetric studies

Thermal denaturation of mAAT was studied by DSC. DSC experiments were performed using a DASM-4 M differential scanning microcalorimeter (Institute for Biological Instrumentation, Pushchino, Russia). All measurements were carried out in 10 mM Na-phosphate, pH 7.5, with 0.5 mM EDTA. The protein solution was heated at a constant rate from 5 to 90 °C and at a constant pressure of 2.2 atm. The reversibility of the thermal transition of mAAT was tested by checking reproducibility of the calorimetric trace during the second heating of the sample immediately after cooling. The calorimetric traces of mAAT were corrected for instrumental background and possible aggregation artefacts by subtracting the scans obtained from the second heating of the samples. Calorimetric traces obtained at various scanning rates were corrected for the instrumental time-response according to Mayorga and Freire [15]. The temperature dependence of the excess heat capacity ( $C_p^{\text{ex}}$ ) was further analyzed and plotted using Origin software (MicroCal Inc.).

We analyzed the temperature profiles of the excess heat capacity assuming that denaturation of mAAT proceeds as an irreversible reaction of the first order:



where N and D are the native and denatured form of the protein, respectively, and  $k_{\text{den}}$  is the denaturation rate constant.

To describe the dependence  $C_p^{\text{ex}}$  on temperature, we used the following equation system [16–18]:

$$\begin{cases} \frac{d\gamma_{\text{nat}}}{dT} = -\frac{k_{\text{den}}\gamma_{\text{nat}}}{v} \\ C_p^{\text{ex}} = Q_t \frac{k_{\text{den}}\gamma_{\text{nat}}}{v} \end{cases}, \quad (2)$$

where  $\gamma_{\text{nat}}$  is the portion of the native protein,  $T$  is the absolute temperature,  $v$  is the temperature scanning rate and  $Q_t$  is the total heat of denaturation. It is assumed that the temperature dependence of the  $k_{\text{den}}$  value (in min<sup>-1</sup>) follows the Arrhenius equation:

$$k_{\text{den}} = \exp\left\{\frac{E_a^{\text{den}}}{R}\left(\frac{1}{T_1^{\text{den}}} - \frac{1}{T}\right)\right\}, \quad (3)$$

where  $E_a^{\text{den}}$  is the energy of activation,  $T_1^{\text{den}}$  is the temperature at which the rate constant  $k_{\text{den}}$  equals 1 min<sup>-1</sup> and  $R$  is the gas constant.

### 2.5. Determination of portions of inactivated and aggregated mAAT

The enzyme was transferred into 10 mM Na-phosphate buffer, pH 7.5, with 0.5 mM EDTA by careful dialysis. Samples containing appropriate amounts of protein were incubated at a well-defined temperature in silicone-covered glass tubes. Each tube was removed at an appropriate time interval, immediately placed in the ice water bath and then centrifuged for 20 min at 20,000 g. Residual enzyme activity was measured at 25 °C as described above. Sample of the unheated protein served as a control. In addition to determination of the enzyme activity we measured the optical density (OD) of the supernatant at 280 nm. The portion of the aggregated protein ( $\gamma_{\text{agg}}$ ) was calculated as  $(1 - \text{OD}/\text{OD}_0)$ , where  $\text{OD}_0$  is the optical density of the initial solution.

### 2.6. DLS studies

For light scattering measurements a commercial instrument Photocor Complex was used (Photocor Instruments Inc., USA; [www.photocor.com](http://www.photocor.com)). A He–Ne laser (Coherent, USA, Model 31-2082, 632.8 nm, 10 mW) was used as a light source. The temperature of sample cell was controlled by the proportional integral derivative (PID) temperature controller to within  $\pm 0.1$  °C. The quasi-cross

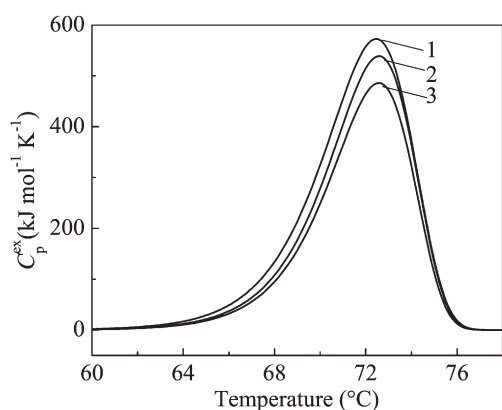


**Fig. 1.** Thermal denaturation of mAAT studied by DSC. Temperature dependence of excess heat capacity ( $C_p^{\text{ex}}$ ) of mAAT (10 mM Na-phosphate buffer, 0.5 mM EDTA, pH 7.5) obtained at various concentrations of the protein: (1) 0.2, (2) 1.0 and (3) 3.2 mg mL<sup>-1</sup>.  $C_p^{\text{ex}}$  was calculated per dimer of mAAT with molecular mass of 91.2 kDa [5]. The heating rate was 1 °C min<sup>-1</sup>.

correlation photon counting system with two photomultiplier tubes (PMT) was used to increase the accuracy of particle sizing in the range from 1.0 nm to 5.0 μm. DLS data have been accumulated and analyzed with multifunctional real-time correlator Photocor-FC that has both logarithmic multiple-tau and linear time-scale modes. DynaLS software (Alango, Israel) was used for polydisperse analysis of DLS data.

The diffusion coefficient  $D$  of the particles is directly related to the decay rate  $\tau_c$  of the time-dependent correlation function for the light-scattering intensity fluctuations:  $D = 1/2\tau_c k^2$ . In this equation  $k$  is the wave number of the scattered light,  $k = (4\pi n/\lambda)\sin(\theta/2)$ , where  $n$  is the refractive index of the solvent,  $\lambda$  is the wavelength of the incident light in a vacuum and  $\theta$  is the scattering angle. The mean hydrodynamic radius of the particles,  $R_h$ , can then be calculated according to the Stokes–Einstein equation:  $D = k_B T / 6\pi\eta R_h$ , where  $k_B$  is Boltzmann's constant,  $T$  is the absolute temperature and  $\eta$  is the shear viscosity of the solvent.

To carry out DLS measurements at a constant heating rate, a fast thermostat has been developed [19]. The fast thermostat was fully controlled with the existing PID controller through the macro procedure of the Photocor program.

Thermal aggregation of mAAT was studied in 10 mM Na-phosphate buffer, pH 7.5, when heating the enzyme solution at a constant rate (1 °C min<sup>-1</sup>). The scattering light was collected at 90° scattering angle and the accumulation time of the autocorrelation function was 30 s.

The dimensionless polydispersity index PI, which is a measure of the broadness of the distribution of particles by size, was calculated according to International standard ISO 13321 [20].

When analyzing the temperature dependences of the hydrodynamic radius for protein aggregation under the regime wherein the protein solution is heated at a constant rate [21,22], we showed that the initial parts of these dependences are described by the linear equation:

$$R_h = R_{h,0} \left[ 1 + \frac{1}{\Delta T_{2R}} (T - T_0) \right], \quad (4)$$

where  $R_{h,0}$  is the hydrodynamic radius of the start aggregates,  $T_0$  is the temperature at which the start aggregates come to view and  $\Delta T_{2R}$  is the temperature interval over which the hydrodynamic radius increases from  $R_{h,0}$  to twice this value. The reciprocal value of parameter  $\Delta T_{2R}$  characterizes the rate of aggregation. The higher the  $1/\Delta T_{2R}$  value, the higher the aggregation rate.

## 2.7. Calculations

Origin 7.0 software (OriginLab Corporation, USA) and Scientist (MicroMath, Inc., USA) software were used for the calculations.

To characterize the degree of agreement between the experimental data and calculated values, we used the coefficient of determination  $R^2$  (without considering the statistical weight of the measurement results) [23]:

$$R^2 = \frac{\sum_{i=1}^{i=n} (Y_i^{\text{obs}} - \bar{Y}^{\text{obs}})^2 - \sum_{i=1}^{i=n} (Y_i^{\text{obs}} - Y_i^{\text{calc}})^2}{\sum_{i=1}^{i=n} (Y_i^{\text{obs}} - \bar{Y}^{\text{obs}})^2}, \quad (5)$$

where  $\bar{Y}^{\text{obs}} = \frac{1}{n} \sum_{i=1}^{i=n} Y_i$  is the average of the experimental data ( $Y_i^{\text{obs}}$ ),  $Y_i^{\text{calc}}$  is the theoretically calculated value of the function  $Y$  and  $n$  is the number of measurements.

## 3. Results

### 3.1. Thermal denaturation of mAAT

DSC analysis shows that thermal denaturation of mAAT is fully irreversible. The heat sorption curve is represented by a sharp thermal transition (Fig. 1). The maximum of mAAT thermal transition ( $T_{\text{max}}$ ) remains constant at variation of the protein concentration in the interval from 0.2 to 3.2 mg mL<sup>-1</sup> (Fig. 1). Some discrepancies between the curves are connected with an experimental error in heat sorption measurements and are acceptable in the calorimetric studies. Consequently, the mechanism of mAAT denaturation does not involve a kinetically significant stage of reversible dissociation of the protein dimer into monomers (see for discussion [18,24]).

Fig. 2 shows the temperature dependences of  $C_p^{\text{ex}}$  for mAAT denaturation obtained at various temperature scanning rates ( $v = 0.25, 0.5, 1.0$  and  $2.0$  °C min<sup>-1</sup>). The position of maximum on the DSC profiles was shifted from 69.7 to 73.1 °C as the temperature scanning rate increased from 0.25 to 2.0 °C min<sup>-1</sup>. Analysis of the DSC data showed that the DSC profiles might be satisfactorily described by the two-state model (Eq. (2)). The values of the total heat denaturation  $Q_t$  and parameters of the Arrhenius equation obtained from analysis of the individual DSC profiles using Eqs. (2) and (3) are given in Table 1. The average value of  $Q_t$  was equal to  $3020 \pm 50$  kJ mol<sup>-1</sup>. The average values of parameters  $E_a^{\text{den}}$  and  $T_i^{\text{den}}$  calculated from simultaneous treatment of all DSC profiles were found to be  $516.6 \pm 0.7$  kJ mol<sup>-1</sup> and  $346.44 \pm 0.01$  K, respectively.

Table 1 shows the standard deviations for parameters  $Q_t$ ,  $E_a^{\text{den}}$  and  $T_i^{\text{den}}$  obtained for fitting of the DSC data to the corresponding theoretical equations using the SCIENTIST program. The low value of standard deviation for parameter  $T_i^{\text{den}}$  shows that this parameter is sensitive to the slightest perturbations. It should be noted that the

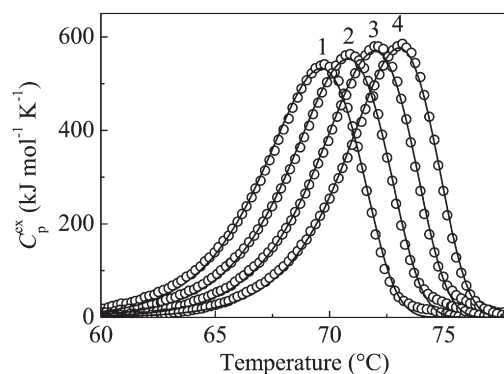


**Fig. 2.** Quantitative analysis of the temperature dependence of  $C_p^{\text{ex}}$  for mAAT (1.5 mg mL<sup>-1</sup>) obtained at various temperature scanning rates: (1) 0.25, (2) 0.5, (3) 1.0 and (4) 2.0 °C min<sup>-1</sup>. Points are the experimental data. The solid curves were calculated from Eqs. (2) and (3) at the following values of parameters:  $E_a^{\text{den}} = 516.6$  kJ/mol and  $T_i^{\text{den}} = 346.44$  K.

**Table 1**

Arrhenius equation parameter estimates for one-step model (1) of thermal denaturation of mAAT

$v, ^\circ\text{C min}^{-1}$	$Q_d, \text{kJ mol}^{-1}$	$E_a^{\text{den}}, \text{kJ mol}^{-1}$	$T_1^{\text{den}}, \text{K}$	$R^2$
0.25	2971 $\pm$ 3	470.6 $\pm$ 0.5	347.24 $\pm$ 0.01	0.9984
0.5	3058 $\pm$ 3	477.9 $\pm$ 0.6	346.90 $\pm$ 0.01	0.9983
1	3079 $\pm$ 4	492.2 $\pm$ 0.6	346.55 $\pm$ 0.01	0.9984
2	2971 $\pm$ 2	519.7 $\pm$ 0.5	346.12 $\pm$ 0.01	0.9992
Fitting to all curves		516.6 $\pm$ 0.7	346.44 $\pm$ 0.01	0.9896

errors indicated in Table 1 represent only the errors of fitting. We did not calculated the errors connected with the other procedures (experimental uncertainties in protein concentration, baseline correction and so on), since the corresponding methods are lacking.

### 3.2. Thermal inactivation of mAAT

Thermal inactivation of mAAT was irreversible at all temperatures studied. Activity could not be recovered by prolonged incubation of partially inactivated samples at 25  $^\circ\text{C}$ .

The study of thermal inactivation of mAAT at various concentrations of the protein (Fig. 3) shows that the kinetics of inactivation is independent of the protein concentration. Effect of temperature on the kinetics of thermal inactivation of mAAT was studied at the enzyme concentration of 0.1 mg mL $^{-1}$ . As can be seen from Fig. 4, the dependences of the relative enzyme activity ( $A/A_0$ ) on time ( $t$ ) are linear in the coordinates  $\{\ln(A/A_0); t\}$  ( $A_0$  and  $A$  are the values of the initial and current enzyme activity). This means that the kinetics of inactivation follows the exponential law:

$$A/A_0 = \exp(-k_{\text{in}}t), \quad (6)$$

where  $k_{\text{in}}$  is the inactivation rate constant.

To describe the dependence of the rate constant  $k_{\text{in}}$  (in min $^{-1}$ ) on temperature, we used the Arrhenius equation:

$$k_{\text{in}} = \exp\left\{\frac{E_a^{\text{in}}}{R} \left(\frac{1}{T_1^{\text{in}}} - \frac{1}{T}\right)\right\}, \quad (7)$$

where  $E_a^{\text{in}}$  is the activation energy for the inactivation process and  $T_1^{\text{in}}$  is the temperature at which  $k_{\text{in}}$  is 1 min $^{-1}$ . Parameters  $E_a^{\text{in}}$  and  $T_1^{\text{in}}$  were determined from the  $\ln k_{\text{in}}$  versus  $1/T$  plot (the line 1, Fig. 5):  $E_a^{\text{in}}$  and  $T_1^{\text{in}}$  are equal to 405.4 $\pm$ 1.5 kJ mol $^{-1}$  and 345.99 $\pm$ 0.02 K, respectively ( $R^2=0.9998$ ). The line 2 in Fig. 5 shows the dependence of  $\ln k_{\text{den}}$  on  $1/T$  calculated from the DSC data. As can be seen from this figure, in the

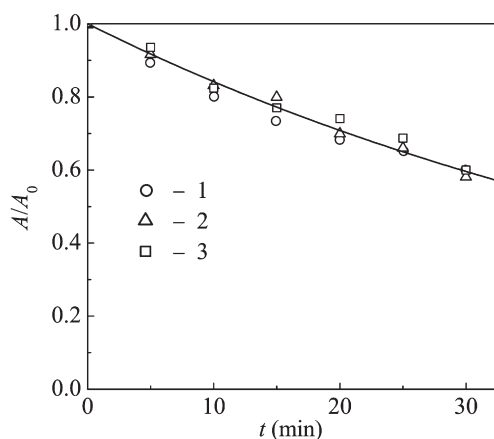


**Fig. 3.** Kinetics of thermal inactivation of mAAT (0.1 mg mL $^{-1}$ ; 10 mM Na-phosphate buffer, 0.5 mM EDTA, pH 7.5; 55  $^\circ\text{C}$ ). The dependence of the relative enzymatic activity of mAAT ( $A/A_0$ ) on time obtained at various concentrations of the enzyme: (1) 0.05, (2) 0.1 and (3) 0.2 mg mL $^{-1}$ .  $A_0$  and  $A$  are the initial and current values of the enzymatic activity.

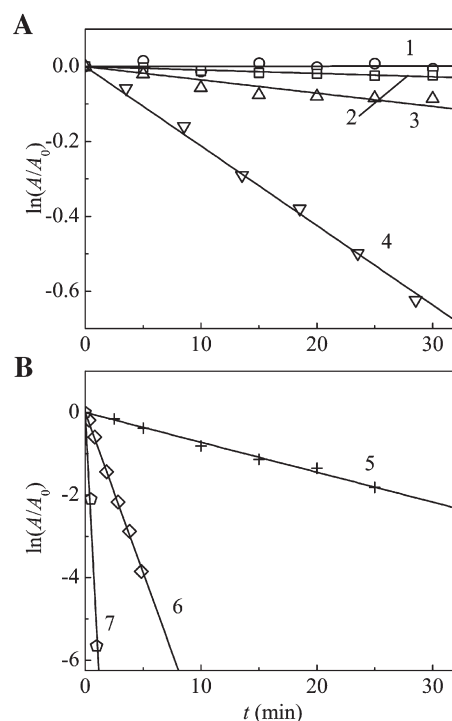


**Fig. 4.** Effect of temperature on the kinetics of inactivation of mAAT (0.1 mg mL $^{-1}$ ). The dependence of the relative enzymatic activity of mAAT ( $A/A_0$ ) on time in semi-logarithmic coordinates obtained at various temperatures of incubation: (1) 50, (2) 52, (3) 57.5, (4) 61, (5) 65, (6) 68, (7) 72 and (7) 77  $^\circ\text{C}$ .

temperature interval under study (from 57.5 to 77  $^\circ\text{C}$ ) the inactivation rate constant exceeds the denaturation rate constant. The  $k_{\text{in}}/k_{\text{den}}$  ratio decreases with temperature from 28.8 $\pm$ 0.1 at 57.5  $^\circ\text{C}$  to 1.30 $\pm$ 0.09 at 77  $^\circ\text{C}$ . Thus, Fig. 5 demonstrates that thermal inactivation of mAAT proceeds faster than thermal denaturation of the enzyme.

### 3.3. Relationship between aggregation, inactivation and denaturation of mAAT

Denaturation of mAAT is accompanied by aggregation of the protein. The portion of the aggregated protein ( $\gamma_{\text{agg}}$ ) was determined by measuring the absorbance of the heated protein solution after centrifugation at 20000 g as described in the section Materials and Methods. Fig. 6A and B show the dependence of  $\gamma_{\text{agg}}$  on time at temperatures 60 and 70  $^\circ\text{C}$ , respectively. These Figures also show the dependences of the portions of the inactivated ( $\gamma_{\text{in}}$ ) and denatured ( $\gamma_{\text{den}}$ ) protein calculated from the

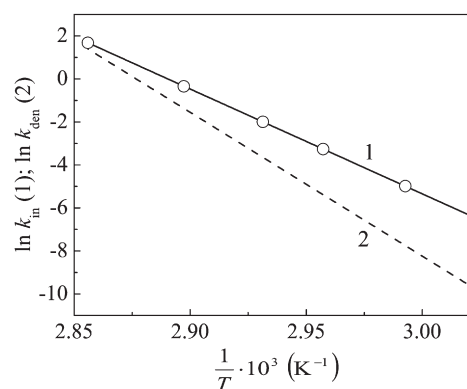


**Fig. 5.** Comparison of the rates of inactivation and denaturation of mAAT. The temperature dependences of the inactivation rate constant ( $k_{\text{in}}$ ; line 1) and the denaturation rate constant ( $k_{\text{den}}$ ; line 2) in the Arrhenius coordinates. Points on the line 1 are the experimental values of  $k_{\text{in}}$ . Dimensions of  $k_{\text{in}}$  and  $k_{\text{den}}$  are given in min $^{-1}$ .



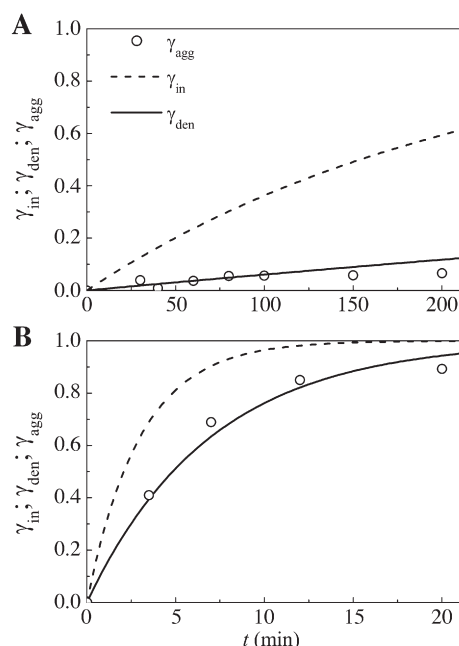


**Fig. 6.** Comparison of the kinetics of accumulation of the aggregated protein with the kinetics of inactivation and denaturation of mAAT ( $0.2 \text{ mg mL}^{-1}$ ) at 60 and 70 °C (A and B, respectively).  $\gamma_{\text{den}}$ ,  $\gamma_{\text{in}}$  and  $\gamma_{\text{agg}}$  are the portions of the denatured, inactivated and aggregated proteins, respectively.

equations  $\gamma_{\text{in}} = [1 - \exp(-k_{\text{in}}t)]$  and  $\gamma_{\text{den}} = [1 - \exp(-k_{\text{den}}t)]$ , respectively, at the following values of  $k_{\text{in}}$  and  $k_{\text{den}}$ :  $k_{\text{in}} = 0.0044$  and  $0.31 \text{ min}^{-1}$  at 60 and 70 °C and  $k_{\text{den}} = 0.00024$  and  $0.082 \text{ min}^{-1}$  at 60 and 70 °C, respectively. As can be seen from Fig. 6, the accumulation of the aggregated mAAT coincides completely with denaturation of the protein. Based on this fact, one may conclude that faster inactivation of mAAT in comparison with denaturation is not due to the capture of the native enzyme by the formed aggregates.

### 3.4. Aggregation of mAAT studied by DLS

Thermal aggregation of mAAT ( $0.2 \text{ mg mL}^{-1}$ , 10 mM Na-phosphate buffer, pH 7.5) was studied under the regime wherein the temperature was elevated in the interval from 45 to 80 °C at the constant rate of  $1 \text{ °C min}^{-1}$ . DLS allows measuring the size of particles formed in the course of protein aggregation. The distributions of protein aggregates by size obtained at various temperatures are represented in Fig. 7. It can be observed that the distribution of aggregates by size is unimodal, and the

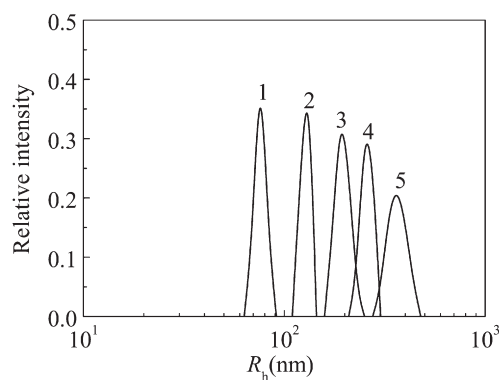
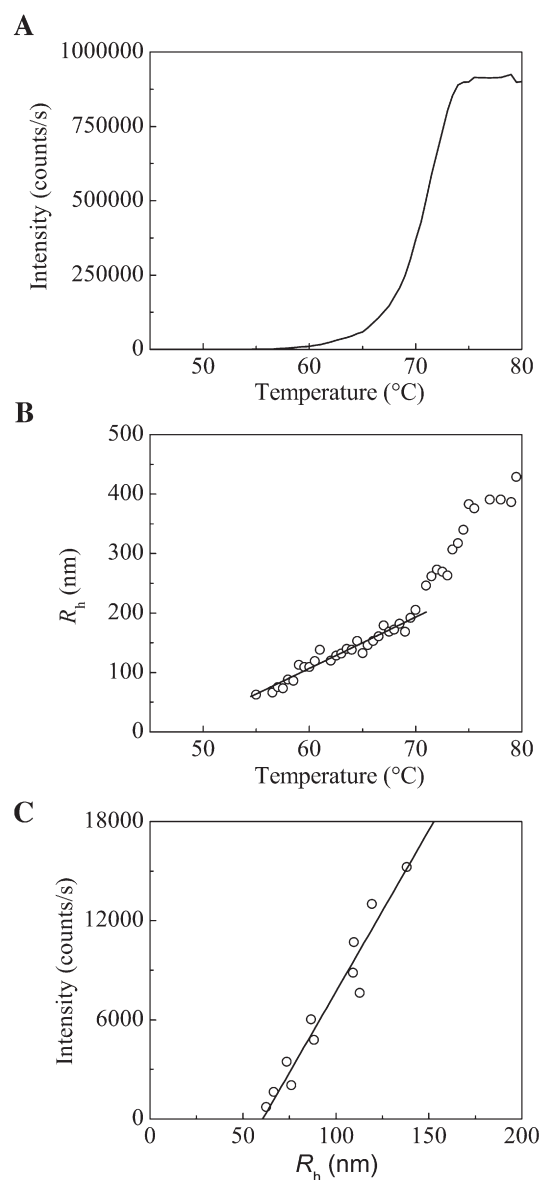


**Fig. 7.** Thermal aggregation of mAAT ( $0.2 \text{ mg mL}^{-1}$ ) registered by DLS under the regime wherein the temperature was elevated at a constant rate ( $1 \text{ °C min}^{-1}$ ). Distributions of the particles by size were obtained at the following temperatures: (1) 55, (2) 63, (3) 69.5, (4) 71 and (5) 75 °C.

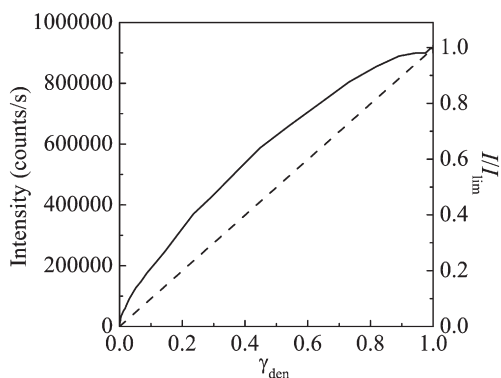
hydrodynamic radius  $R_h$  of aggregates changes towards higher values with the temperature. The elevation of temperature is also accompanied by a wider distribution of particles by size. The polydispersity index PI was  $0.09 \pm 0.02$  at 70.5 °C and increased to  $0.82 \pm 0.04$  at 76.5 °C.

Fig. 8 shows the dependences of the light scattering intensity ( $I$ ) and hydrodynamic radius ( $R_h$ ) on temperature (panels A and B, respectively). The light scattering intensity increases with temperature and reaches the limiting value at about 75 °C. Before analyzing the dependence of the hydrodynamic radius on time, we constructed the light scattering intensity versus the hydrodynamic radius plot (Fig. 8, panel C). The relationship between  $I$  and  $R_h$  is linear. The length on the abscissa axis cut off by the straight line corresponds to the hydrodynamic radius of the start aggregates ( $R_{h,0}$ ), which are registered at the instant the initial increase in the light scattering intensity is observed. The  $R_{h,0}$  value was found to be  $60 \pm 1 \text{ nm}$ .

The initial part of the dependence of the hydrodynamic radius on temperature is linear (Fig. 8B). Thus, Eq. (4) may be used for



**Fig. 8.** Aggregation of mAAT ( $0.4 \text{ mg mL}^{-1}$ ) heated at a constant rate of  $1 \text{ °C min}^{-1}$ . (A and B) The dependences of the light scattering intensity and the hydrodynamic radius ( $R_h$ ) on temperature. (C) The light scattering intensity versus the hydrodynamic radius plot.



**Fig. 9.** Relationship between denaturation and aggregation of mAAAT heated at a constant rate ( $1\text{ }^{\circ}\text{C min}^{-1}$ ). The light scattering intensity (the data presented in Fig. 8A) versus the portion of the denatured protein ( $\gamma_{\text{den}}$ ) plot. The right ordinate axis is the normalized value of the light scattering intensity  $I/I_{\text{lim}}$  ( $I$  is the light scattering intensity and  $I_{\text{lim}}$  is the limiting value of  $I$  at  $\gamma_{\text{den}}=1$ ). The dotted line corresponds to the case of strict correlation between the light scattering intensity and the portion of the denatured protein ( $\gamma_{\text{den}}=I/I_{\text{lim}}$ ). The values of  $\gamma_{\text{den}}$  are calculated from Eq. (8).

determination of the parameter  $T_0$  (the temperature, at which the start aggregates appear) and parameter  $\Delta T_{2R}$  (the temperature interval, over which the hydrodynamic radius increases from  $R_{h,0}$  to  $2R_{h,0}$ ):  $T_0=54.6\pm 0.5\text{ }^{\circ}\text{C}$  and  $\Delta T_{2R}=7.04\pm 0.4\text{ }^{\circ}\text{C}$ . The parameter  $T_0$  is the length on the horizontal line corresponding to the level  $R_h=R_{h,0}$  cut off by the straight line.

### 3.5. Relationship between aggregation measured by the increase in the light scattering intensity and denaturation of mAAAT

To compare the time-course of the denaturation and aggregation processes registered under the regime wherein the temperature was elevated at a constant rate, we have constructed the increment of the light scattering intensity characterizing mAAAT aggregation versus the portion of the denatured protein plot (Fig. 9). Before proceeding to construction of such a plot, we calculated the portion of the denatured protein ( $\gamma_{\text{den}}$ ) as a function of temperature at the temperature scanning rate of  $1\text{ }^{\circ}\text{C min}^{-1}$  using the following equation system:

$$\left\{ \begin{array}{l} \frac{d\gamma_{\text{den}}}{dT} = \frac{k_{\text{den}}(1-\gamma_{\text{den}})}{v} \\ k_{\text{den}} = \exp\left\{ \frac{E_{\text{a}}^{\text{den}}}{R} \left( \frac{1}{T_1^{\text{den}}} - \frac{1}{T} \right) \right\} \end{array} \right. \quad (8)$$

Parameters  $E_{\text{a}}^{\text{den}}$  and  $E_{\text{a}}^{\text{den}}$  were set equal to  $516.6\text{ kJ mol}^{-1}$  and  $346.44\text{ K}$ , respectively.

The extrapolation of the light scattering intensity to  $\gamma_{\text{den}}=1$  gives, on the above plot, the limiting value of the light scattering intensity, which is attained at high temperatures (in the region of about  $75\text{ }^{\circ}\text{C}$ ):  $I_{\text{lim}}=850000\text{ counts s}^{-1}$ . Knowing the  $I_{\text{lim}}$  value, we can normalize the light scattering intensity values. As seen from Fig. 9, the  $I/I_{\text{lim}}$  values are ahead of the  $\gamma_{\text{den}}$  values. In other words, the aggregation process “overruns” denaturation of mAAAT.

## 4. Discussion

The following model may be proposed to describe the discrepancy between the rates of inactivation and denaturation of mAAAT. The model involves the stage of inactivation of mAAAT:  $E_{\text{a}} \rightarrow E_{\text{in}}$  ( $E_{\text{a}}$  and  $E_{\text{in}}$  are the active and inactive forms of mAAAT, respectively). We assume that enzyme inactivation is due to local structural alterations in the active site, the conformation of the protein globule remaining practically unchanged. Besides, we propose that the enthalpy change for the conversion between the active and inactive enzyme forms is very low, although the activation energy for the conversion is

significant. Otherwise this stage would be manifested in the DSC profiles.

Since according to our assumption the conformations of  $E_{\text{a}}$  and  $E_{\text{in}}$  forms are similar, denaturation of these forms proceeds with the same rate. In other words, irreversible denaturation of  $E_{\text{a}}$  and  $E_{\text{in}}$  forms is characterized by the same denaturation rate constant  $k_{\text{den}}$ :



where  $E_{\text{den}}$  is the denatured form of the enzyme.

It is evident that scheme (9) is equivalent to the one-stage model of denaturation (see scheme (1)). Thus, the proposed model of mAAAT inactivation-denaturation explains the one-stage mechanism of mAAAT denaturation and the higher rate of the enzyme inactivation in comparison with the denaturation rate.

One of the possible schemes of mAAAT inactivation-denaturation may be that where only the inactive form ( $E_{\text{in}}$ ) undergoes irreversible denaturation:  $E_{\text{a}} \xrightarrow{k_{\text{in}}} E_{\text{in}} \xrightarrow{k_{\text{den}}} E_{\text{den}}$ . We tried to describe the DSC profiles of mAAAT obtained at various scanning rates (Fig. 2) in the frame of this scheme using the mathematical apparatus elaborated by Lyubarev et al. [25]. The obvious discordance was observed between the experimental and calculated data. Thus, the two-stage model of denaturation  $E_{\text{a}} \rightarrow E_{\text{in}} \rightarrow E_{\text{den}}$  is unacceptable for description of mAAAT denaturation.

Thus, according to the DSC data, denaturation of mAAAT proceeds as an irreversible monomolecular reaction (scheme (1)). The quantitative analysis of the temperature profiles of  $C_p^{\text{ex}}$  allowed us to estimate the parameters of the Arrhenius equation ( $E_{\text{a}}^{\text{den}}$  and  $T_1^{\text{den}}$ ). The values of the activation energy for protein denaturation following the one-stage irreversible model have been summarized in the reviews [18,26,27]. The DSC data were used in these calculations. The maximum values of the activation energy are about  $530\text{--}650\text{ kJ mol}^{-1}$  (for example, for acetylcholinesterase [28], annexin V E17G [29], cellulase [30], 5-enolpyruvate shikimate-3-phosphate synthase [31]). The value of  $E_{\text{a}}^{\text{den}}$  for thermal denaturation of mAAAT was found to be  $516.6\text{ kJ mol}^{-1}$ . Consequently, mAAAT belongs to the group of proteins characterized by the maximum values of the energy of activation for the denaturation process.

The study of aggregation of mAAAT heated at a constant rate ( $1\text{ }^{\circ}\text{C min}^{-1}$ ) by DLS has shown that the initial stage of protein aggregation is the stage of formation of the start aggregates. The hydrodynamic radius of the start aggregates ( $R_{h,0}$ ) may be determined from the light scattering intensity versus the hydrodynamic radius plot. The  $R_{h,0}$  value was found to be  $60\pm 1\text{ nm}$ . The kinetics of mAAAT aggregation is consistent with the mechanism of thermal aggregation of proteins developed by us previously [19,21,22,32–36]. The mechanism involves the stage of formation of the start aggregates (the primary clusters). Further sticking of the start aggregates and aggregates of higher order proceeds under the regime of diffusion-limited cluster–cluster aggregation (DLCA). The fulfillment of this regime means that each collision results in the sticking of the interacting particles. The fact that the initial part of the dependence of the hydrodynamic radius of mAAAT protein aggregates on temperature is a straight line agrees with DLCA regime of aggregation [21,36]. The parameter  $T_0$  (the temperature at which the start aggregates are registered) may be considered as an “initial temperature of aggregation”. For mAAAT  $T_0=54.6\pm 0.5\text{ }^{\circ}\text{C}$ . For glyceraldehyde-3-phosphate dehydrogenase and glycogen phosphorylase *b* from rabbit muscle we obtained the values of  $T_0$  equal to  $45.4\pm 0.2\text{ }^{\circ}\text{C}$  [21] and  $49.7\pm 0.2\text{ }^{\circ}\text{C}$  [22], respectively.

DSC data on denaturation and DLS data on aggregation of mAAAT were obtained under the regime wherein the temperature was

elevated at a constant rate. This circumstance allows us to compare the increase in the light scattering intensity in the course of aggregation with the degree of denaturation of mAAT. In the case of thermal aggregation of glyceraldehyde-3-phosphate dehydrogenase we observed a linear correlation between the increase in the light scattering intensity and the portion of the denatured protein [19]. However, there is no linear correlation between the light scattering intensity and the portion of the denatured protein ( $\gamma_{\text{den}}$ ) for mAAT. The normalized  $I$  values ( $I/I_{\text{lim}}$ ) exceed the  $\gamma_{\text{den}}$  values.

## 5. Conclusion

Comparison of the rate of inactivation and the rate of denaturation of mAAT clearly demonstrates that inactivation is ahead of denaturation of the enzyme, the difference between the rates of inactivation and denaturation becoming especially noticeable when temperature decreases. These results are consistent with the idea by Tsou that the enzyme active site is more fragile and more easily perturbed than the protein molecule as a whole [37–42]. The high fragility of the active site of mAAT in comparison with the stability of the whole protein globule may be due to the location of the active site in the region of the contact of the subunits. Relatively small alterations of the mutual arrangement of the subunits may result in dramatic changes in the spatial organization of the active site and loss of catalytic power.

According to Lawton and Doonan [10], irreversibility of thermal inactivation of mAAT is due to formation of an altered conformation of the enzyme and not a result of irreversible chemical changes. This conclusion supports our view that faster inactivation of mAAT in comparison with unfolding of the protein globule is due to local temperature-induced rearrangements of the active site of the enzyme.

## Acknowledgements

This study was funded by the Russian Foundation for Basic Research (grants 08-04-00666-a and 06-04-39008), the Program “Molecular and Cell Biology” of the Presidium of the Russian Academy of Sciences and State Scientific Programme Republic of Belarus “Biological Engineering and Biosafety”.

We are thankful to A. Lyubarev for the valuable comments.

## References

- [1] J.W. Boyd, The intracellular distribution, latency and electrophoretic mobility of L-glutamate-oxaloacetate transaminase from rat liver, *Biochem. J.* 81 (1961) 434–441.
- [2] C.A. McPhalen, M.G. Vincent, D. Picot, J.N. Jansonius, A.M. Lesk, C. Chothia, Domain closure in mitochondrial aspartate aminotransferase, *J. Mol. Biol.* 227 (1992) 197–213.
- [3] G.C. Ford, G. Eichele, J.N. Jansonius, Three-dimensional structure of a pyridoxal-phosphate-dependent enzyme, mitochondrial aspartate aminotransferase, *Proc. Natl. Acad. Sci. U. S. A.* 77 (1980) 2559–2563.
- [4] E. Sandmeier, P. Christen, Mitochondrial aspartate aminotransferase 27/32–410. Partially active enzyme derivative produced by limited proteolytic cleavage of native enzyme, *J. Biol. Chem.* 255 (1980) 10284–10289.
- [5] N. Feliss, M. Martinez-Carrión, The molecular weight and subunits of the isozymes of glutamic aspartic transaminase, *Biochem. Biophys. Res. Commun.* 40 (1970) 932–940.
- [6] S. Doonan, F. Martini, S. Angelaccio, S. Pascarella, D. Barra, F. Bossa, The complete amino acid sequences of cytosolic and mitochondrial aspartate aminotransferases from horse heart, and inferences on evolution of the isoenzymes, *J. Mol. Evol.* 23 (1986) 328–335.
- [7] S.M. West, N.C. Price, The unfolding and refolding of cytoplasmic aspartate aminotransferase from pig heart, *Biochem. J.* 261 (1989) 189–196.
- [8] S.M. West, N.C. Price, The unfolding and attempted refolding of mitochondrial aspartate aminotransferase from pig heart, *Biochem. J.* 265 (1990) 45–50.
- [9] C.M. Twomey, S. Doonan, A comparative study of the thermal inactivation of cytosolic and mitochondrial aspartate aminotransferases, *Biochim. Biophys. Acta* 1342 (1997) 37–44.
- [10] J.M. Lawton, S. Doonan, Thermal inactivation and chaperonin-mediated renaturation of mitochondrial aspartate aminotransferase, *Biochem. J.* 334 (1998) 219–224.
- [11] A. Azzariti, R.A. Vacca, S. Giannattasio, R.S. Merafina, E. Marra, S. Doonan, Kinetic properties and thermal stabilities of mutant forms of mitochondrial aspartate aminotransferase, *Biochim. Biophys. Acta* 1386 (1998) 29–38.
- [12] D. Barra, F. Bossa, S. Doonan, H.M. Fahmy, F. Martini, G.J. Hughes, Large-scale purification and some properties of the mitochondrial aspartate aminotransferase from pig heart, *Eur. J. Biochem.* 64 (1976) 519–526.
- [13] G.L. Peterson, Determination of total protein, *Methods Enzymol.* 91 (1983) 95–119.
- [14] A. Karmen, A note on the spectrometric assay of glutamic-oxalacetic transaminase in human blood serum, *J. Clin. Invest.* 34 (1955) 131–133.
- [15] O.L. Mayorga, E. Freire, Dynamic analysis of differential calorimetric data, *Biophys. Chem.* 87 (1987) 87–96.
- [16] B.I. Kurganov, A.E. Lyubarev, J.M. Sanchez-Ruiz, V.L. Shnyrov, Analysis of differential scanning calorimetry data for proteins. Criteria of validity of one-step mechanism of irreversible protein denaturation, *Biophys. Chem.* 69 (1997) 125–135.
- [17] A.E. Lyubarev, B.I. Kurganov, V.N. Orlov, H.M. Zhou, Two-state irreversible thermal denaturation of muscle creatine kinase, *Biophys. Chem.* 79 (1999) 199–204.
- [18] B.I. Kurganov, A.E. Lyubarev, Study of irreversible thermal denaturation of proteins by differential scanning calorimetry, in: E.A. Permyakov, V.N. Uversky (Eds.), *Methods in Protein Structure and Stability Analysis: Conformational Stability, Size, Shape and Surface of Protein Molecules*, Nova Science Publishers Inc., New York, 2007, pp. 109–145.
- [19] K.A. Markossian, H.A. Khanova, S.Y. Kleimenov, D.I. Levitsky, N.A. Chebotareva, R.A. Asryants, V.I. Muronetz, L. Saso, I.K. Yudin, B.I. Kurganov, Mechanism of thermal aggregation of rabbit muscle glyceraldehyde-3-phosphate dehydrogenase, *Biochemistry* 45 (2006) 13375–13384.
- [20] International standard ISO 13321: 1996(E), Particle size analysis-Photon correlation spectroscopy, International Organization for Standardization, Geneva, 1996.
- [21] H.A. Khanova, K.A. Markossian, S.Y. Kleimenov, D.I. Levitsky, N.A. Chebotareva, N.V. Golub, R.A. Asryants, V.I. Muronetz, L. Saso, I.K. Yudin, B.I. Kurganov, Effect of alpha-crystallin on thermal denaturation and aggregation of rabbit muscle glyceraldehyde-3-phosphate dehydrogenase, *Biophys. Chem.* 125 (2007) 521–531.
- [22] A.V. Meremyanin, T.B. Eronina, N.A. Chebotareva, S.Y. Kleimenov, I.K. Yudin, K.O. Muranov, M.A. Ostrovsky, B.I. Kurganov, Effect of alpha-crystallin on thermal aggregation of glycogen phosphorylase b from rabbit skeletal muscle, *Biochemistry (Moscow)* 72 (2007) 518–528.
- [23] Scientist for Experimental Data Fitting, Microsoft Windows Version 2.0, MicroMath, Inc., Salt Lake City, 1995.
- [24] J.M. Sanchez-Ruiz, Theoretical analysis of Lumry-Eyring models in differential scanning calorimetry, *Biophys. J.* 61 (1992) 921–935.
- [25] A.E. Lyubarev, B.I. Kurganov, A.A. Burlakova, V.N. Orlov, Irreversible thermal denaturation of uridine phosphorylase from *Escherichia coli* K-12, *Biophys. Chem.* 70 (1998) 247–257.
- [26] B.I. Kurganov, A.E. Lyubarev, Study of irreversible thermal denaturation of proteins by differential scanning calorimetry, *Uspekhi Biol. Khim. (Moscow)* 40 (2000) 43–84.
- [27] B.I. Kurganov, A.E. Lyubarev, Analysis of DSC data relating to proteins undergoing irreversible thermal denaturation, *J. Therm. Anal. Cal.* 62 (2000) 51–62.
- [28] D.I. Kreimer, V.L. Shnyrov, E. Villar, I. Silman, L. Weiner, Irreversible thermal denaturation of Torpedo californica acetylcholinesterase, *Protein Sci.* 4 (1995) 2349–2357.
- [29] T. Vogl, C. Jatzke, H.J. Hinz, J. Benz, R. Huber, Thermodynamic stability of annexin V E17G: equilibrium parameters from an irreversible unfolding reaction, *Biochemistry* 36 (1997) 1657–1668.
- [30] A.L. Garda-Salas, R.I. Santamaria, M.J. Marcos, G.G. Zhadan, E. Villar, V.L. Shnyrov, Differential scanning calorimetry of the irreversible thermal denaturation of cellulase from *Streptomyces halstedii* JM8, *Biochem. Mol. Biol. Int.* 38 (1996) 161–170.
- [31] E.K. Merabet, M.C. Walker, H.K. Yuen, J.A. Sikorski, Differential scanning calorimetric study of 5-enolpyruvyl shikimate-3-phosphate synthase and its complexes with shikimate-3-phosphate and glyoxylate: irreversible thermal transitions, *Biochim. Biophys. Acta* 1161 (1993) 272–278.
- [32] H.A. Khanova, K.A. Markossian, B.I. Kurganov, A.M. Samoilov, S.Y. Kleimenov, D.I. Levitsky, I.K. Yudin, A.C. Timofeeva, K.O. Muranov, M.A. Ostrovsky, Mechanism of thermal aggregation of betaA-crystallin by alpha-crystallin, *Biochemistry* 44 (2005) 15480–15487.
- [33] K.A. Markossian, B.I. Kurganov, D.I. Levitsky, H.A. Khanova, N.A. Chebotareva, A.M. Samoilov, T.B. Eronina, N.V. Fedurkina, L.G. Mitskevich, A.V. Meremyanin, S.Yu. Kleymenov, V.F. Makeeva, V.I. Muronets, I.N. Naletova, I.N. Shalova, R.A. Asryants, E.V. Schmalhausen, L. Saso, Yu.V. Panyukov, E.N. Dobrov, I.K. Yudin, A.C. Timofeeva, K.O. Muranov, M.A. Ostrovsky, Mechanisms of chaperone-like activity, in: T.R. Obalinsky (Ed.), *Protein Folding: New Research*, Nova Science Publishers Inc., New York, 2006, pp. 89–171.
- [34] Y. Panyukov, I. Yudin, V. Drachev, E. Dobrov, B. Kurganov, The study of amorphous aggregation of tobacco mosaic virus coat protein by dynamic light scattering, *Biophys. Chem.* 127 (2007) 9–18.
- [35] N. Golub, A. Meremyanin, K. Markossian, T. Eronina, N. Chebotareva, R. Asryants, V. Muronets, B. Kurganov, Evidence for the formation of start aggregates as an initial stage of protein aggregation, *FEBS Lett.* 581 (2007) 4223–4227.
- [36] A.V. Meremyanin, T.B. Eronina, N.A. Chebotareva, B.I. Kurganov, Kinetics of thermal aggregation of glycogen phosphorylase b from rabbit skeletal muscle. Mechanism of protective action of alpha-crystallin, *Biopolymers* 89 (2008) 124–134.
- [37] C.L. Tsou, Location of the active sites of some enzymes in limited and flexible molecular regions, *Trends Biochem. Sci.* 11 (1986) 427–429.
- [38] Y.Z. Lin, S.J. Liang, J.M. Zhou, C.L. Tsou, P.Q. Wu, Z.K. Zhou, Comparison of inactivation and conformational changes of D-glyceraldehyde-3-phosphate dehydrogenase during thermal denaturation, *Biochim. Biophys. Acta* 1038 (1990) 247–252.
- [39] Y.L. Zhang, J.M. Zhou, C.L. Tsou, Inactivation precedes conformation change during thermal denaturation of adenylate kinase, *Biochim. Biophys. Acta* 1164 (1993) 61–67.
- [40] C.L. Tsou, Conformational flexibility of enzyme active sites, *Science* 262 (1993) 380–381.
- [41] C.L. Tsou, Active site flexibility in enzyme catalysis, *Ann. N. Y. Acad. Sci.* 864 (1998) 1–8.
- [42] C.L. Tsou, The role of active site flexibility in enzyme catalysis, *Biochemistry (Moscow)* 63 (1998) 253–258.